

# Thermodynamic Treatment of Undercooled Cu-Mg Liquid and the Limits for Partitionless Crystallization

S.H. Zhou and R.E. Napolitano

(Submitted June 14, 2006)

The thermodynamic properties of the binary Cu-Mg system are examined with a focus on equilibria involving the liquid phase, which is described with a four-species association model, incorporating a two-state treatment for the pure component liquids below their respective melting temperatures. The terminal and intermediate crystalline phases are described as substitutional solid solutions, employing two sublattices for the latter. Model parameters are fitted using available experimental data, and the resulting phase diagram is reported over the full range of compositions in the binary system. We also report the associated  $T_0$  curves, indicating the limits of partitionless crystallization and compare these with reports of amorphous solid formation during rapid solidification processing.

**Keywords** phase equilibria, two-state model, undercooled liquid

## 1. Introduction

The properties of highly undercooled liquids play an essential role in the various phenomena that occur during rapid solidification processing, including nucleation of stable or crystalline phases, the selection of growth morphologies under high-driving forces, non-equilibrium chemical partitioning at high-growth rates, and the formation of glassy phases. As thermodynamic and kinetic criteria are developed to predict or describe these processes,<sup>[1,2]</sup> it is essential to develop thermodynamic models which accurately describe the energetics of undercooled liquids and the associated phase equilibria.

In a previous paper,<sup>[3]</sup> we modeled the thermodynamic properties and associated phase equilibria for the Cu-Mg binary system and compared the resulting phase diagram with the prior thermodynamic modeling reported by Coughanowr et al.<sup>[4]</sup> and by Zou and Chang.<sup>[5]</sup> While those results are consistent with reported experimental data,<sup>[6-29]</sup> we point out that the SGTE parameters<sup>[30]</sup> are not sufficient for describing the behavior of undercooled liquids. This is clearly indicated in Fig. 1, where the heat capacities of the pure Cu and Mg liquids, calculated using these parameters, show a discontinuity in their first derivative at  $T_m$ . This unrealistic behavior is also exhibited by our previous treatment of the alloy liquid, as shown in Fig. 2 for the  $\text{Cu}_{14.4}\text{Mg}_{85.5}$  composition. To address this problem here, we

incorporate a two-state model<sup>[31,32]</sup> into our prior approach<sup>[3]</sup> to describe the thermodynamic properties of the undercooled liquids and to compute the relevant phase equilibria and limits for partitionless crystallization from the melt. We employ a CALPHAD<sup>[33,34]</sup> methodology, where the model parameters describing the Gibbs free energies associated with the formation of compounds or solution phases are determined through a systematic semi-empirical optimization, using available experimental data from calorimetry, x-ray diffraction, electron-probe microchemical analysis, and optical micrography.<sup>[6-29]</sup>

## 2. Thermodynamic Models

We adopt our previously reported approach<sup>[3]</sup> for the modeling of Gibbs free energies and associated phase equilibria for the Cu-Mg binary system, but we add a two-state treatment<sup>[31,32]</sup> of the undercooled elemental liquids. Thermodynamic functions for other pure element states are taken from the SGTE database,<sup>[30]</sup> as listed in Table 1. An association model<sup>[35,36]</sup> is used for the alloy liquid, and sublattice models<sup>[37]</sup> are employed for the solid phases. All thermodynamic models are defined in Table 2, where the total Gibbs free energy for any phase,  $\phi$ , is generally given by the sum of three contributions,

$$G_m^\phi = {}^{\text{ref}}G_m^\phi + {}^{\text{id}}G_m^\phi + {}^{\text{xs}}G_m^\phi, \quad (\text{Eq 1})$$

where the subscript,  $m$ , indicates that all terms are molar quantities. The first term in Eq. 1 is the sum of occupancy-weighted sublattice end-member contributions. The second and third terms are the ideal and excess parts of the Gibbs free energy of mixing, respectively. In Table 2, we list the Redlich-Kister formalism for the excess term for the fcc and hcp solid solutions. It should be noted, however, that for this work we use only the first term ( $j = 0$ ) with a constant coefficient (i.e. regular solution). The specific treatment of each phase is discussed briefly here.

S.H. Zhou, and R.E. Napolitano, Materials & Engineering Physics Program, Ames Laboratory, USDOE, Iowa State University, 116 Wilhelm Hall, Ames, IA 50011, USA; R.E. Napolitano, Department of Materials Science and Engineering, Iowa State University, 116 Wilhelm Hall, Ames, IA 50011, USA; Contact e-mail: ralphn@iastate.edu

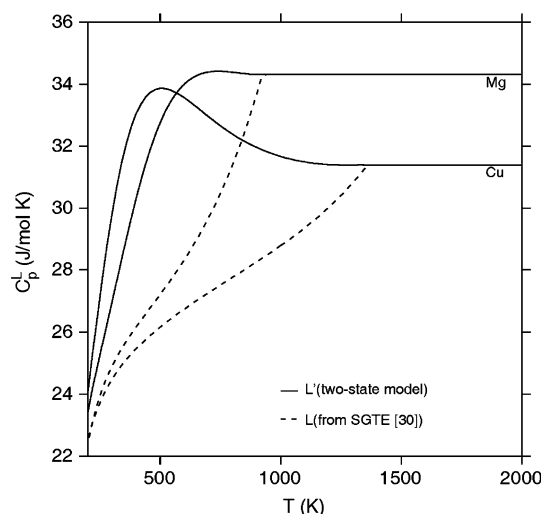


Fig. 1 Heat capacities for the pure component liquids

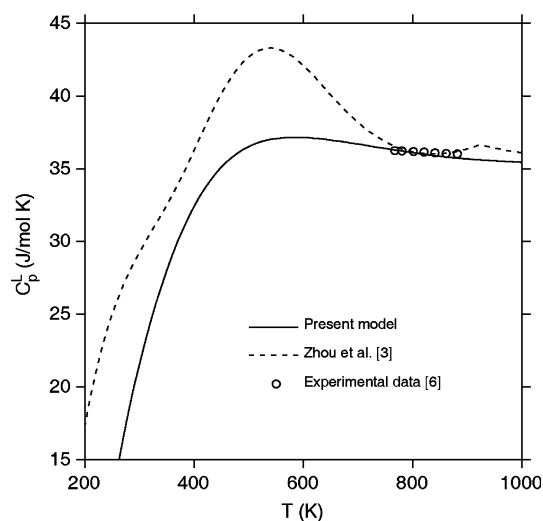


Fig. 2 The heat capacity for the liquid  $\text{Cu}_{1.4.5}\text{Mg}_{85.5}$

We employ a four-species association model,<sup>[35,36]</sup> for the binary liquid solution (L) where  $\text{Cu}_2\text{Mg}$  and  $\text{CuMg}_2$  are chosen as the relevant intermediate chemical associates according to previously reported experimental data,<sup>[38]</sup> as we have discussed elsewhere.<sup>[3]</sup> The Gibbs free energy of an intermediate chemical associate,  $\text{Cu}_m\text{Mg}_n$ , is given as

$${}^0G_{\text{Cu}_m\text{Mg}_n}^{\text{L}} = m{}^0G_{\text{Cu}}^{\text{L}} + n{}^0G_{\text{Mg}}^{\text{L}} + \Delta G_{\text{Cu}_m\text{Mg}_n}^{\text{L}}, \quad (\text{Eq } 2)$$

where the Gibbs free energy of formation,  $\Delta G_{\text{Cu}_m\text{Mg}_n}^{\text{L}}$ , for the indicated species is assumed to have temperature dependence of the general form,

$$a_0 + a_1T + a_2T \ln T + a_3T^2 + a_4T^3 + a_5T^4 + a_6T^{-1} + a_7T^{-9}. \quad (\text{Eq } 3)$$

To address the problem discussed earlier regarding the discontinuity in the heat capacity of the liquid phase,<sup>[3]</sup> we

employ a two-state approach,<sup>[31,32]</sup> describing the liquid phase (L) as an ideal mixture of low-free energy “solid-like” particles and high-free energy “liquid-like” particles. Accordingly, for a single component, the molar Gibbs free energy of the mixture is written as

$$G_m^{\text{L}} = (1-f){}^0G_m^{\text{sol}} + f{}^0G_m^{\text{liq}} + RT[(1-f) \ln(1-f) + f \ln f], \quad (\text{Eq } 4)$$

where  $f$  is the mole fraction of atoms associated with the liquid-like particles.  ${}^0G_m^{\text{sol}}$  and  ${}^0G_m^{\text{liq}}$  are the molar Gibbs free energies of “solid-like” and “liquid-like” particles, respectively. An equilibrium population of states is assumed, such that the fraction of atoms in the activated or “liquid-like” state is simply found by minimizing  $G_m^{\text{L}}$ , yielding

$$f_{\text{eq}} = \frac{e^{-\varepsilon/RT}}{1 + e^{-\varepsilon/RT}}, \quad (\text{Eq } 5)$$

where the activation energy is given by  $\varepsilon = {}^0G_m^{\text{liq}} - {}^0G_m^{\text{sol}}$ . Substituting Eq 5 into Eq 4 gives the Gibbs free energy of the mixture, referenced to the low-energy solid-like phase,

$$G_m^{\text{L}} = {}^0G_m^{\text{sol}} - RT \ln(1 + e^{-\varepsilon/RT}). \quad (\text{Eq } 6)$$

The task of modeling  $G_m^{\text{L}}$  for any component, therefore, entails only the selection of appropriate “liquid-like” and “solid-like” Gibbs free energy states,  ${}^0G_m^{\text{sol}}$  and  ${}^0G_m^{\text{liq}}$ , each as a function of temperature. We allow for the general temperature dependence in a definition of the “solid-like” state with respect to a perfectly crystalline reference,

$${}^0G_m^{\text{sol}} = {}^0G_i^{\text{S}} + \Delta G_m^{\text{sol}}, \quad (\text{Eq } 7)$$

where  ${}^0G_i^{\text{S}}$  is the Gibbs free energy of either Cu(fcc) or Mg(hcp), and where we assume that  $\Delta G_m^{\text{sol}}$  takes the general form given in Eq 3, with only the first four coefficients being nonzero. Finally, we adopt Agren’s<sup>[31,32]</sup> simplification of the temperature dependence of  $\varepsilon$ , defining the activation energy simply as

$$\varepsilon_i = {}^0L_i^{\text{liq}} - RT, \quad (i = \text{Cu or Mg}), \quad (\text{Eq } 8)$$

where we assume that  ${}^0L_i^{\text{liq}}$  is a constant. Thus, with the stated assumptions, the two-state model is completely described by Eq 6-8, along with Eq 3, where the parameters left for evaluation are  $a_0$ ,  $a_1$ ,  $a_2$ ,  $a_3$  and  ${}^0L_i^{\text{liq}}$  for each component. This parameter set was evaluated for Cu, by Agren et al.,<sup>[32]</sup> while those for Mg are determined in the current work, as indicated in Table 1.

All crystalline phases are treated as substitutional solid solutions. The fcc and hcp phases are treated with a single lattice, using the models given in Table 2. The intermetallic phases,  $\text{Cu}_2\text{Mg-C}_{15}$  and  $\text{Mg}_2\text{Cu-C}_b$ , are described as two-sublattice solid solutions of the form  $(\text{Cu}, \text{Mg})_2(\text{Cu}, \text{Mg})_1$ . The associated Gibbs free energies are modeled as shown in Table 2. Given this sublattice formulation, each of the two structures ( $C_{15}$  and  $C_b$ ) can assume four different stoichiometries ( $\text{Cu}_2\text{Cu}$ ,  $\text{Mg}_2\text{Cu}$ ,  $\text{Cu}_2\text{Mg}$ , and  $\text{Mg}_2\text{Mg}$ ), with only one being that of the stable compound (i.e.  $\text{Cu}_2\text{Mg-C}_{15}$  and  $\text{Mg}_2\text{Cu-C}_b$ ). For these compounds, we express  ${}^0G_{\text{Cu}_m\text{Mg}_n}^{\text{C}_{15}}$  and  ${}^0G_{\text{Mg}_m\text{Cu}_n}^{\text{C}_b}$  using the temperature dependent form given in Eq 3

Section I: Basic and Applied Research

**Table 1 Thermodynamic parameters for the pure components (J/mol)**

	${}^0G_{Cu}^L$	${}^0G_{Cu}^L$	${}^0G_{Cu}^{fcc}$	${}^0G_{Cu}^{hcp}$
Ref	[32]	[30]		
$T_{min}$	298	1357.77	298	1357.77
$T_{max}$	1357.77	3200	1357.77	3200
${}^0G^{ref}$	${}^0G_{Cu}^{fcc}$	...	...	${}^0G_{Cu}^{fcc}$
$a_0$	7985	-46.545	-7770.458	-13542.026
$a_1$	...	173.881484	130.485235	183.803828
$a_2$	...	-31.38	-24.112392	-31.38
$a_3$	$1.0135 \times 10^{-4}$	...	$-2.65684 \times 10^{-3}$	...
$a_4$	...	...	$1.29223 \times 10^{-7}$	...
$a_5$	...	...	...	...
$a_6$	...	...	52478	...
$a_7$	...	...	...	$3.64167 \times 10^{29}$
$\epsilon$	10609.70325-RT	...	...	...
Ref	This work	[30]		
$T_{min}$	298	923	298	298
$T_{max}$	923	3000	3000	923
${}^0G^{ref}$	${}^0G_{Mg}^{hcp}$	...	${}^0G_{Mg}^{hcp}$	...
$a_0$	5341.2729	-5439.869	2600	-8367.34
$a_1$	8.7659	195.324057	-0.9	143.675547
$a_2$	-2.2124526	-34.3088	...	-26.1849782
$a_3$	$3.5278263 \times 10^{-3}$	...	...	$4.858 \times 10^{-4}$
$a_4$	...	...	...	$-1.393669 \times 10^{-6}$
$a_5$	...	...	...	...
$a_6$	...	...	...	78950
$a_7$	...	...	...	...
$\epsilon$	15014.169-RT	...	...	$1.038192 \times 10^{28}$

**Table 2 Summary of the thermodynamic models used for the Cu-Mg binary system**

Phase	Method	Formulation	Model
Liquid	Association model	(Cu, Cu <sub>2</sub> Mg, CuMg <sub>2</sub> ,Mg)	${}^{ref}G_m^L = \sum_i x_i {}^0G_i^L$ ${}^{id}G_m^L = RT \sum_i x_i \ln x_i$ ${}^{xs}G_m^L = \sum_i \sum_{j>i} x_i x_j {}^0L_{ij}^L$ (i,j = Cu,Cu <sub>2</sub> Mg, CuMg <sub>2</sub> , Mg)
Cu(fcc) Mg(hcp)	One-sublattice model	(Cu,Mg) <sub>1</sub>	${}^{ref}G_m^\phi = \sum_{i=Cu,Mg} x_i {}^0G_i^\phi$ ${}^{id}G_m^\phi = RT \sum_{i=Cu,Mg} x_i \ln x_i$ ${}^{xs}G_m^\phi = x_{Cu} x_{Mg} \sum_{j=0}^n {}^jL_{Cu,Mg}^\phi (x_{Cu} - x_{Mg})^j$
Cu <sub>2</sub> Mg(-C <sub>15</sub> ) CuMg <sub>2</sub> (-C <sub>b</sub> )	Two-sublattice model	(Cu,Mg) <sub>2</sub> (Cu,Mg) <sub>1</sub>	${}^{ref}G_m^\phi = \sum_{i=Cu,Mg} y_i^I \sum_{j=Cu,Mg} y_j^{II} {}^0G_{ij}^\phi$ ${}^{id}G_m^\phi = RT \sum_{i=Cu,Mg} (2y_i^I \ln y_i^I + y_i^{II} \ln y_i^{II})$ ${}^{xs}G_m^\phi = y_{Cu}^I y_{Mg}^I \sum_{i=Cu,Mg} y_i^{II} \sum_{k=0}^k {}^kL_{Cu,Mg;i}^\phi (y_{Cu}^I - y_{Mg}^I)^k$ $+ y_{Cu}^{II} y_{Mg}^{II} \sum_{i=Cu,Mg} y_i^I \sum_{k=0}^k {}^kL_{i;Cu,Mg}^\phi (y_{Cu}^{II} - y_{Mg}^{II})^k$

and leave the indicated coefficients for evaluation (see Table 3) based on available enthalpy of formation, melting temperature, and heat capacity data, as we have previously

discussed.<sup>[3]</sup> For the unstable compounds (i.e. Cu<sub>2</sub>Cu-C15, Mg<sub>2</sub>Cu-C<sub>15</sub>, Mg<sub>2</sub>Mg-C<sub>15</sub>, Cu<sub>2</sub>Cu-C<sub>b</sub>, Cu<sub>2</sub>Mg-C<sub>b</sub>, and Mg<sub>2</sub>Mg-C<sub>b</sub>), there are no available heat capacity data with

**Table 3** Ground state standard Gibbs free energy parameters (see Table 2) for the intermetallic phases

${}^0G_{ij}^0$	${}^0G_{Cu:Mg}^{C_{15}}$ , J/mol		${}^0G_{Mg:Cu}^{C_b}$ , J/mol	
$T_{min}$ , K	298	1070	298	850
$T_{max}$ , K	1070	6000	850	6000
$a_0$	-58201	-65262.18413	-53491	-57610.6334
$a_1$	409.542	490.8219613	425.468	480.2433846
$a_2$	-76.1	-87.17102875	-77.9913484	-85.33353573
$a_3$	$-9.9 \times 10^{-4}$	...	$2.31 \times 10^{-3}$	...
$a_4$	183906	...	190378	...
$a_5$	$-1.35 \times 10^{-6}$	...	$-2.72115 \times 10^{-6}$	...
$a_6$	...	...	...	...
$a_7$	...	...	...	...

which to evaluate the temperature dependence. Therefore, we express the Gibbs free energy as

$${}^0G_{A_2B}^\phi = 2{}^0G_A^\phi + {}^0G_B^\phi + \Delta G_{A_2B}^\phi, \quad (A, B = Cu, Mg) \quad (\text{Eq 9})$$

where  ${}^0G_A^\phi$  and  ${}^0G_B^\phi$  are the molar Gibbs free energies of either fcc-Cu or hcp-Mg, and  $\Delta G_{A_2B}^\phi$  is the Gibbs free energy of formation of the indicated end-member.

In total, in addition to the standard SGTE parameters for the pure elements, our treatment employs five (5) parameters for the two-state model for each undercooled elemental liquid (Table 1), one (1) temperature dependent standard Gibbs free energy for each of the two-stable intermetallic end members (Table 3), ten (10) binary interaction parameters (Table 4), and eight (8) Gibbs free energy of formation parameters (Table 4), two of which are temperature dependent. The evaluation of these parameters is discussed in the following section.

**Table 4** Thermodynamic model parameters (see Table 2) determined for the Cu-Mg system (per mole of formula unit)

Phase (model)	Parameters	Value, J/mol	Ref
Liquid (Cu, Cu <sub>2</sub> Mg, CuMg <sub>2</sub> , Mg)	$\Delta G_{Cu_2Mg_1}^L$	$-28312 + 9.595T$	This work
	$\Delta G_{Cu_1Mg_2}^L$	$-80122 + 435.088T$	
		$-56.1847 \ln(T)$	
		$+ 0.010087T^2$	
		$+ 469990T^{-1}$	
	${}^0L_{Cu,Mg}^L$	-22611	
	${}^0L_{Cu,Cu_2Mg}^L$	-20012	
	${}^0L_{Cu_2Mg,Mg}^L$	-25845	
	${}^0L_{Cu,CuMg_2}^L$	-24230	
	${}^0L_{CuMg_2,Cu_2Mg}^L$	0	
Hcp (Cu,Mg)	${}^0L_{CuMg_2,Mg}^{hcp}$	0	[3]
	${}^0L_{Cu,Mg:Va}^{hcp}$	39230	
Fcc (Cu,Mg)	${}^0L_{Cu,Mg:Va}^{fcc}$	-19345	
Cu <sub>2</sub> Mg-C <sub>15</sub> (Cu, Mg) <sub>2</sub> (Cu, Mg)	$\Delta G_{Cu:Cu}^{C_{15}}$	46500	This work
	$\Delta G_{Mg:Cu}^{C_{15}}$	104160	
	$\Delta G_{Mg:Mg}^{C_{15}}$	21000	
	${}^0L_{Cu:Cu,Mg}^{C_{15}}$	-27868	
	${}^0L_{Cu,Mg:Mg}^{C_{15}}$	3521	
CuMg <sub>2</sub> -C <sub>b</sub> (Cu, Mg) <sub>2</sub> (Cu, Mg)	$\Delta G_{Cu:Cu}^{C_b}$	61170	[3]
	$\Delta G_{CuMg_2}^{C_b}$	116820	
	$\Delta G_{Mg:Mg}^{C_b}$	38760	

### 3. Modeling Results

Expressions for the standard Gibbs free energy ( ${}^0G_i^\phi$ ) of each pure component in the relevant phases are listed in Table 1. Based on the model described in the preceding section and summarized in Table 2, we evaluate the parameters for the undercooled elemental liquid Mg and adopt those developed by Agren et al.<sup>[32]</sup> for pure Cu, as listed in Table 1. To include the influence of our two-state treatment of the undercooled elemental liquids, we re-evaluate the parameters for the liquid solution phase and those for the compounds Cu<sub>2</sub>Mg-C<sub>15</sub> and Mg<sub>2</sub>Cu-C<sub>b</sub>. This is discussed in the remainder of the present section. The other relevant thermodynamic parameters are taken from our earlier work<sup>[3]</sup> as indicated in Table 3 and 4.

To evaluate the parameters of  $G_m^L$ , for the two-state model used for the undercooled liquid Mg, we take the approach described previously<sup>[2]</sup> and apply the conditions

$$\frac{\partial^n G_m^L}{\partial T^n} = \frac{\partial^n G_m^{L'}}{\partial T^n} \quad (n = 0, 1, 2, 3) \quad (\text{Eq 10})$$

at  $T = T_m$ , noting that these conditions simply equate the values of  $G$ ,  $S$ ,  $C_p$ , and  $\partial C_p / \partial T$ , respectively, for  $L$  and  $L'$ . Given that we have four equations and five model parameters, we cannot solve for the parameters explicitly. We temporarily assign  $a_2 = 0$  and use Eq. 10 with  $n = 2$  and  $n = 3$ , where  $a_0$  and  $a_1$  play no role, and solve for the parameter  $a_3$  as a function of  ${}^0L_{Mg}^{liq}$ . Under this constraint, we compute  $C_p^L(T_m)$  vs.  ${}^0L_{Mg}^{liq}$ , as plotted (solid curve) in Fig. 3 and compare with the value of  $C_p^L(T_m)$ . We note that there is no solution for this case (i.e.  $a_2 = 0$ ). Choosing the value of  $C_p^L(T_m)$  associated with the closest approach to  $C_p^L(T_m)$ , we fix both  $a_3$  and  ${}^0L_{Mg}^{liq}$  to the corresponding values. We then relax our constraint on the parameter  $a_2$  and solve for the only single-valued solution to the Eq 10 for  $n = 2$ . The  $C_p^L$  vs.  ${}^0L_{Mg}^{liq}$  curve associated with this non-zero value of  $a_2$  is plotted (broken curve) in Fig. 3. Subsequently, we use Eq 10 with  $n = 1$  and  $n = 0$  to evaluate  $a_1$  and  $a_0$ , respectively. The five parameters for the pure Mg liquid ( $T < T_m$ ), determined in this way, are listed in Table 1. The final modeled heat capacity functions for the pure component liquids, above and below  $T_m$ , are plotted in Fig. 1.

The two-state modeling results for the single-component undercooled liquids are incorporated into the association model described in a previous section. The parameters for the liquid phase are evaluated using reported values of activity,<sup>[21]</sup> chemical potential,<sup>[18-23]</sup> enthalpy of mixing,<sup>[17,18]</sup> and heat capacity<sup>[6]</sup> and are listed in Table 4. The heat capacity of the alloy liquid, as modeled with the two-state approach, exhibits a more realistic behavior than our prior treatment, as shown in Fig. 2. For the solid phases, the model parameters reported by Zhou et al.<sup>[3]</sup> are considered. Due to the modified treatment of the Gibbs free energy for the liquid phase, the  ${}^0G$  and  ${}^0L$  parameters for both stoichiometries Cu<sub>2</sub>Mg-C<sub>15</sub> and Mg<sub>2</sub>Cu-C<sub>b</sub> are re-evaluated using reported experimental data,<sup>[9,10,12]</sup> while the remaining parameters are adopted from Zhou et al.,<sup>[3]</sup> as listed in Table 3 and 4. The calculated enthalpy of mixing and

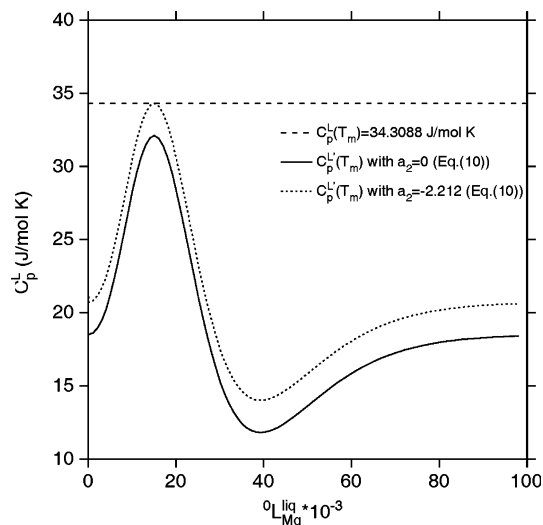


**Fig. 3** The calculated heat capacity for the Mg liquid as a function of the parameter  ${}^0L_{Mg}^{liq}$ , constrained by Eq 10 for  $n = 2, 3$

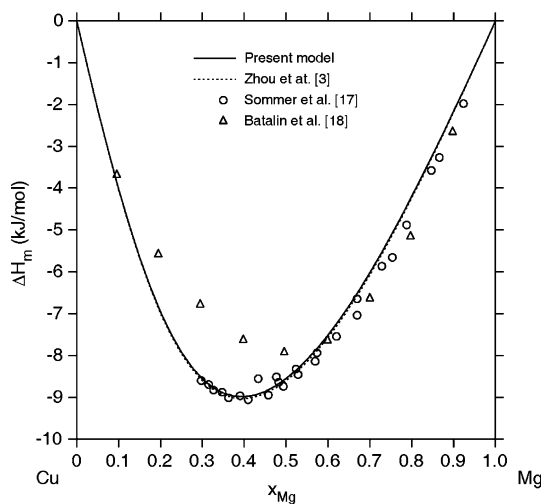


**Fig. 4** The computed enthalpy of mixing for the binary liquid at 1120 K, compared with experimental data

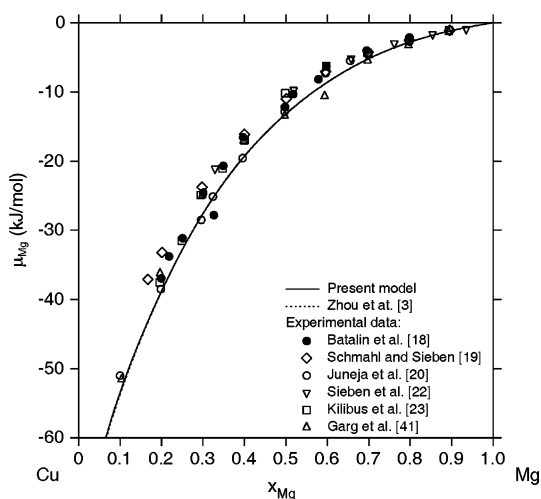


**Fig. 5** The chemical potential of Mg in the binary liquid at 1100 K, computed from the current model as function of composition and compared with experimental data

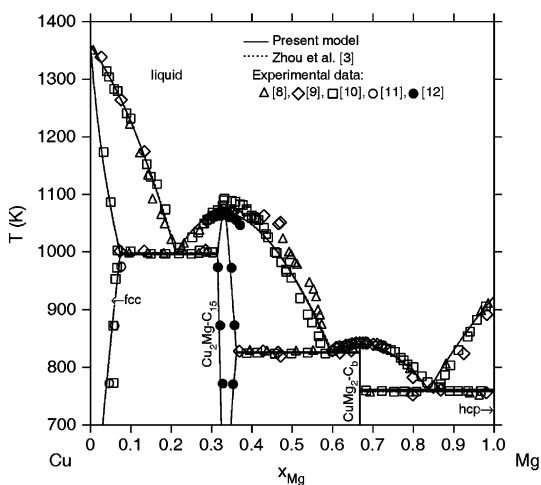


**Fig. 6** The equilibrium Cu-Mg phase diagram, as computed using the present model. Reported experimental data and model are shown for comparison

chemical potential of Mg as a function of composition for the Cu-Mg liquid phase are plotted in Fig. 4 and 5, respectively. The resulting equilibrium phase diagram is plotted in Fig. 6 along with reported experimental data.<sup>[8-12]</sup> The computed invariant reactions are compared with available experimental data in Table 5. In Fig. 7, we plot the liquidus ( $\mu_i^L = \mu_i^\phi$ ) and  $T_0(G_i^L = G_i^\phi)$  curves, showing the relevant criteria for crystallization from the melt with equilibrium chemical partitioning and zero chemical partitioning, respectively. Also shown in this figure are experimental observations of glass formation in this binary system,<sup>[6]</sup> indicating, as previously suggested,<sup>[2]</sup> that  $T_0$  may be a practical limit for partitionless crystallization.

#### 4. Conclusions

Employing a two-state treatment and empirical methods for evaluation of coefficients, the Gibbs free energy vs. composition curves for all relevant phases in the Cu-Mg binary system are modeled, and the associated binary phase diagram is computed. While the reassessed phase diagram does not differ significantly from our previous report, the computed alloy liquid heat capacity, as modeled with the two-state approach, exhibits a more realistic behavior. Combining a two-state model for the pure component liquid reference states in the sub-melting temperature regime and a four-species association model for the liquid solution,

**Table 5 Invariant reactions in the Cu-Mg system**

Reaction	Variable	Calculated results				Experimental data
		This work	[3]	[4]	[5]	
Liq → Cu <sub>2</sub> Mg-C <sub>15</sub>	T, K	1067.5	1066.3	1073.0	1066.2	1063 <sup>[8]</sup> 1070 <sup>[9]</sup> 1092 <sup>[10]</sup> 1066 <sup>[12]</sup>
	x <sub>(liquid,Mg)</sub>	0.333	0.333	0.333	0.333	0.333 <sup>[12]</sup>
Liq → CuMg <sub>2</sub> -C <sub>b</sub>	x <sub>(C<sub>15</sub>,Mg)</sub>	0.333	0.333	0.333	0.333	0.333 <sup>[12]</sup>
	T, K	840.5	840.5	841.0	843.1	841.0 <sup>[10,12]</sup> 0.667 <sup>[12]</sup>
Liq → fcc + Cu <sub>2</sub> Mg-C <sub>15</sub>	x <sub>(liquid,Mg)</sub>	0.667	0.667	0.667	0.667	0.667 <sup>[12]</sup>
	x <sub>(C<sub>b</sub>,Mg)</sub>	0.667	0.667	0.667	0.667	0.667 <sup>[12]</sup>
Liq → fcc + Cu <sub>2</sub> Mg-C <sub>15</sub>	T, K	996.5	998.8	998.8	998.3	995 <sup>[10]</sup> 998 <sup>[8,12]</sup>
	x <sub>(liquid,Mg)</sub>	0.212	0.213	0.209	0.214	0.230 <sup>[8]</sup>
	x <sub>(fcc,Mg)</sub>	0.073	0.074	0.069	0.075	0.069 <sup>[12]</sup>
	x <sub>(C<sub>15</sub>,Mg)</sub>	0.315	0.314	0.313	0.316	0.310 <sup>[12]</sup>
Liq → CuMg <sub>2</sub> -C <sub>b</sub> + Cu <sub>2</sub> Mg-C <sub>15</sub>	T, K	825.6	826.5	825.5	825.2	828 <sup>[8,9]</sup> 825 <sup>[10,12]</sup>
	x <sub>(liquid,Mg)</sub>	0.595	0.594	0.595	0.588	0.585 <sup>[8]</sup>
	x <sub>(C<sub>b</sub>,Mg)</sub>	0.667	0.667	0.667	0.667	0.667 <sup>[8]</sup>
	x <sub>(C<sub>15</sub>,Mg)</sub>	0.361	0.361	0.356	0.359	0.353 <sup>[8]</sup>
Liq → hcp + CuMg <sub>2</sub> -C <sub>b</sub>	T, K	760.1	757.3	759.0	758.0	753 <sup>[8]</sup> 758 <sup>[9,10]</sup>
	x <sub>(liquid,Mg)</sub>	0.839	0.838	0.839	0.841	0.855 <sup>[9,10]</sup>
	x <sub>(hcp,Mg)</sub>	1.000	1.000	1.000	1.000	1 <sup>[10]</sup>
	x <sub>(C<sub>b</sub>,Mg)</sub>	0.667	0.667	0.667	0.667	0.667 <sup>[10]</sup>

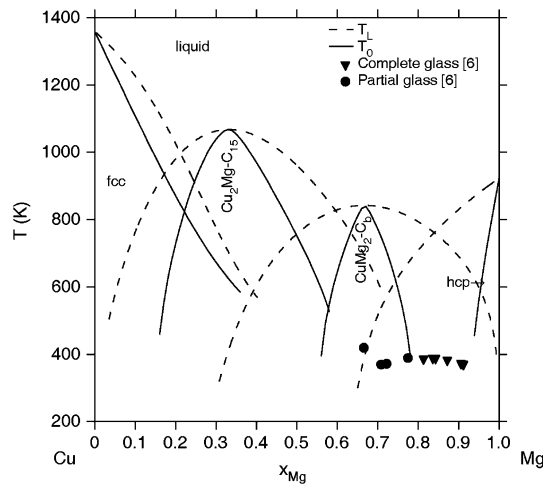


**Fig. 7** The  $T_L$  and  $T_0$  curves calculated using the parameters in Table 1, 3 and 4. Experimental reports of complete and partial glass formation are also shown<sup>[6]</sup>

we compute the values of  $T_L$  and  $T_0$ . Comparison with experimental observations of glass formation in this binary system supports prior claims<sup>[2,39,40]</sup> that, as an upper bound to completely partitionless crystallization from the melt, the  $T_0$  temperature provides a practical limit for the glass formation range.

**Acknowledgments**

This work was performed under the Solidification Science focus area within the Ames Laboratory Materials and Engineering Physics Program and was made possible by support from the Office of Basic Energy Science, Division of Materials Science, U.S. Department of Energy, under Contract No. W7405-Eng-82.

**References**

1. A.W. Zhu, G.J. Shiflet, and D.B. Miracle, Glass Forming Ranges of Al-rare Earth Metal Alloys: Thermodynamic and Kinetic Analysis, *Scripta Mater.*, 2004, **50**, p 987-991
2. S.H. Zhou and R.E. Napolitano, Phase Equilibria and Thermodynamic Limits for Partitionless Crystallization in the Al-La Binary System, *Acta Mater.*, 2006, **54**, p 831-840
3. S.H. Zhou, Y. Wang, F.G. Shi, F. Sommer, L.-Q. Chen, Z.-K. Liu, and R. E. Napolitano, Modeling of Thermodynamic Properties and Phase Equilibria for the Cu-Mg Binary System, *J. Phase Equilib.*, 2006, **28**, Printing
4. C.A. Coughanowr, I. Ansara, R. Luoma, M. Hamalainen, and H.L. Lukas, Ni. Assessment of the Cu-Mg System, *Z. Metallk.*, 1991, **82**, p 574-581
5. Y. Zou and Y.A. Chang, Thermodynamic Calculation of the Mg-Cu Phase Diagram, *Z. Metallk.*, 1993, **84**, p 662-667
6. F. Sommer, G. Bucher, and B. Predel, Thermodynamic Investigations of Mg-Cu and Mg-Ni Metallic Glasses, *J. Phys. Colloq. C*, 1980, **8**, p 563-566

## Section I: Basic and Applied Research

7. G. Grime and W. Morris-Jones, An x-ray Investigation of the Copper-Magnesium Alloys, *Phil. Mag.*, 1929, **7**, p 1113-1134
8. G.G. Urazova, *Zh. Russ. Fiz-Khim. Obschestva*, 1907, **39**, p 1556-1581
9. R. Sahmen, Metallographic Announcements from the Institute for Inorganic Chemistry of the University of Gottingen LVIII Concerning the Alloys of Copper with Cobalt, Iron, Manganese and Magnesium, *Z. Anorg. Chem.*, 1908, **57**, p 1-33
10. W.R.D. Jones, The Copper-Magnesium Alloys. Part IV. The Equilibrium Diagram, *J. Inst. Met.*, 1931, **46**, p 395-419
11. I.L. Rogelberg, *T Gos Nauchn Issled.*, 1957, **16**, p 82-89
12. P. Bagnoud and P. Feschotte, Binary Systems Mg-Cu and Mg-Ni, Particularly the Non-Stoichiometry of the MgCu<sub>2</sub> and MgNi<sub>2</sub> Laves Phases, *Z. Metallkd.*, 1978, **69**, p 114-120
13. M. Hansen, *J. Inst. Met.*, 1927, **37**, p 93-100
14. N.I. Stepanov and I.I. Kornilov, *Izv. Inst. Fiz-Khim.*, 1935, **7**, p 89-98
15. A.S. Yue, and R.S. Pierre eds., *Metall. Soc. Conf.*. Interscience Publishers Inc, New York, 1961, p 613-615
16. J.W. Jenkin, *J. Inst. Met.*, 1927, **37**, p 100-101
17. F. Sommer, J.J. Lee, and B. Predel, Calorimetric Investigations of Liquid Alkaline Earth Metal Alloys, *Ber. Bunsenges. Phys. Chem.*, 1983, **87**, p 792-797
18. G.I. Batalin, V.S. Sudavtsova, and M.V. Mikhailovskaya, Thermodynamic Properties of Liquid Alloys of the Cu-Mg Systems, *Izv. V.U.Z. Tsvetn. Metall.*, 1987, **2**, p 9-31
19. N.G. Schmahl and P. Sieben, *NPL Symposium 9 on Phys Chem of Metallic Solutions and Intermetallic Compounds*. HMSO, London, 1958, p 1-16
20. J.M. Juneja, G.N.K. Iyengar, and K.P. Abraham, Thermodynamic Properties of Liquid (Magnesium + Copper) Alloys By Vapor-Pressure Measurements Made By a Boiling-Temperature Method, *J. Chem. Thermodyn.*, 1986, **18**, p 1025-1035
21. S.P. Garg, Y.J. Bhatt, and C.V. Sundaram, Thermodynamic Study of Liquid Cu-Mg Alloys by Vapour Pressure Measurements, *Metall. Trans.*, 1973, **4**, p 283-289
22. P. Sieben and N.G. Schmahl, *Giesserei*, 1966, **18**, p 197-201
23. A.V. Klibus, *Trans. Inst. Met. Severdlosk.*, 1969, **18**, p 55-62
24. H. Feufel and F. Sommer, Thermodynamic Investigations of Binary-Liquid and Solid Cu-Mg and Mg-Ni Alloys and Ternary Liquid Cu-Mg-Ni Alloys, *J. Alloy. Compd.*, 1995, **224**, p 42-54
25. R.C. King and O.J. Kleppa, A Thermochemical Study of Some Selected Laves Phases, *Acta Metall.*, 1964, **12**, p 87-97
26. B. Predel and H. Ruge, Beitrag zur Frage nach den Bindungsverhältnissen in Laves-phasen, *Mater. Sci. Eng.*, 1972, **9**, p 333-339
27. M. Arita, Y. Ichinose, and M. Someno, *Thermodynamic Properties of the Ti-Cu, Ti-Ni and Mg-Cu Systems by Metal-Hydrogen Equilibration*. Metall. Soc. AIME, Warrendale, PA, 1981, p 153-158
28. V.N. Eremenko, G.M. Lukashenko, and R.I. Polotskaya, Thermodynamic Properties of Magnesium-Copper Compounds, *Russ. Met.*, 1968, **1**, p 126-129
29. A.T.W. Kempen, H. Nitsche, F. Sommer, and E.J. Mittemeijer, Crystallization Kinetics of Amorphous Magnesium-rich Magnesium-Copper and Magnesium-Nickel Alloys, *Metall. Mater. Trans. Phys. Metall. Mater. Sci.*, 2002, **33**, p 1041-1050
30. A.T. Dinsdale, SGTE Data for Pure Elements, *Calphad*, 1991, **15**, p 317-425
31. J. Agren, No. Thermodynamics of Supercooled Liquids and Their Glass-Transition, *Phys. Chem. Liquids*, 1988, **18**, p 123-139
32. J. Agren, B. Cheynet, M.T. Clavaguera-Mora, K. Hack, J. Hertz, F. Sommer, and U.R. Kattner, Thermodynamic Models and Data for Pure Elements and Other Endmembers of Solutions, *CALPHAD*, 1995, **19**, p 449-480
33. L. Kaufman and H. Bernstein, *Computer Calculation of Phase Diagrams*. Vol. 4, Academic Press, Inc., New York, 1970
34. N. Saunders and A.P. Miodownik, *CALPHAD (Calculation of Phase Diagrams): A Comprehensive Guide*. Pergamon, Oxford, New York, 1998
35. F. Sommer, Association Model for the Description of the Thermodynamic Functions of Liquid Alloys. I.—Basic Concepts, *Z. Metallkd.*, 1982, **73**, p 72-86
36. H.G. Krull, R.N. Singh, and F. Sommer, Generalised Association Model, *Z. Metallk.*, 2000, **91**, p 356-365
37. B. Sundman and J. Agren, A Regular Solution Model for Phases with Several Components and Sublattices, Suitable for Computer Applications, *J. Phys. Chem. Solids*, 1981, **42**, p 297-301
38. W.E. Lukens and C.N.J. Wagner, The Structure of Liquid Cu-Mg Alloys, *Z. Naturforsch. A*, 1973, **28**, p 297-304
39. R.B. Schwarz, P. Nash, and D. Turnbull, The Use of Thermodynamic Model in the Prediction of the Glass-forming Range of Binary Alloys, *J. Mater. Res.*, 1987, **2**, p 456-460
40. P. Nash and R.B. Schwarz, Calculation of the Glass Forming Range in Binary Metallic Systems Using Thermodynamic Models, *Acta Metall.*, 1988, **36**, p 3047-3053